

Contents lists available at ScienceDirect

# Polymer

journal homepage: http://www.elsevier.com/locate/polymer





# Synthesis of site-specific charged metallopolymers via reversible addition-fragmentation chain transfer (RAFT) polymerization

Ye Sha <sup>a,b,\*</sup>, Tianyu Zhu <sup>b</sup>, Md Anisur Rahman <sup>b</sup>, Yujin Cha <sup>b</sup>, Jihyeon Hwang <sup>b</sup>, Zhenyang Luo <sup>a</sup>, Chuanbing Tang <sup>b,\*\*</sup>

- <sup>a</sup> College of Science, Nanjing Forestry University, Nanjing, 210037, PR China
- b Department of Chemistry and Biochemistry, University of South Carolina, Columbia, SC, 29208, United States

## ARTICLE INFO

Keywords:
Reversible addition-fragmentation chain transfer (RAFT)
Metallocene
Cobaltocenium
Metallopolymer

### ABSTRACT

Site-specific cobaltocenium-labeled polymers are synthesized by reversible addition-fragmentation chain transfer (RAFT) polymerization using cobaltocenium-labeled chain transfer agents. These chain transfer agents show counterion-dependent solubility. Based on the chemical structure of the chain transfer agents, single cobaltocenium moieties are dictated to be in predetermined locations at either the center or terminals of the polymer chains. Polymerization of hydrophobic monomers (methyl methacrylate, methyl acrylate and styrene) and hydrophilic monomers (2-(dimethylamino)ethyl methacrylate and methacrylic acid) is demonstrated to follow a controlled manner based on kinetic studies. Cobaltocenium-labeled polymers with molecular weights greater than 100,000 Da can be prepared by using a difunctional chain transfer agent. Photophysical properties, electrochemical properties, thermal properties and morphology of the cobaltocenium-labeled polymers are also investigated.

# 1. Introduction

Metallopolymers show unique functionalities due to the combination of redox, magnetic and catalytic properties dictated by their metal centers and their processability from polymers [1-9]. In the realm of metallopolymer synthesis, metallocenes (either neutral or cationic) act as a type of versatile building block to introduce metal moieties into polymer frameworks [10-12]. From one perspective, metallocenes can be used as the main components with numerous units distributed along the polymer main-chain or side-chains [13–20]. From another perspective, metallocenes can also manifest themselves as multifunctional molecular tools that can be employed at the surface or interface of engineering and biological materials to help elucidate the structure and properties of molecules, which often arise in the form of affinity labels and spectroscopic probes appended to polymer chains. Specifically, a single-unit labeling strategy, as opposed to a multiple labeling strategy, could be used to study the function imparted by a metallocene moiety that is used as a probe and that dictates the single-chain behavior of a polymer, thus providing a promising candidate from which the redox behavior can be accurately reflected [21,22]. Very recently, it was proven that metallocenes can be stress-responsive mechanophores when they are labeled on polymer backbones [23–25]. However, both the labeling quantities and position along the chain should be well defined, usually at the chain terminals, chain centers or junction sites.

In the past decade, site-specific metallocene-containing polymers have been prepared by living radical polymerization methodologies [13, 23,24,26]. However, most of these metal centers are only neutral metallocenes. As a comparison, the realization of positively charged metallocenes, especially cobaltocenium, as a representative of this group, has proven to be very difficult [21]. This difficulty is not only due to the relative lack of synthetic methodology towards functional initiator/monomer derivatives [27,28], but also because of the very different polymerization controllability [21], making the preparation of site-specific charged metallocene-containing polymers nontrivial.

For example, atom transfer radical polymerization (ATRP) can be used to prepare neutral ferrocene-containing and ruthenocene-containing polymers in a well-controlled manner [19,24,29–33]; however, for cationic cobaltocenium, the controllability was only demonstrated to be moderate, largely due to the positively charged metal centers, thus leading to ion exchange with copper salt catalysts [21]. As

E-mail addresses: shaye@njfu.edu.cn (Y. Sha), tang4@mailbox.sc.edu (C. Tang).

 $<sup>^{\</sup>star}$  Corresponding author. College of Science, Nanjing Forestry University, Nanjing, 210037, PR China.

<sup>\*\*</sup> Corresponding author.

a way to circumvent this inevitable counterion exchange problem, reversible addition-fragmentation chain transfer (RAFT) polymerization has been proven to be very robust for side-chain cobaltocenium-containing polymers without the need for copper salts [34–36]. Therefore, we expect that site-specific cobaltocenium-labeled polymers can be prepared via site-specific RAFT polymerization where cobaltocenium-containing chain transfer agents (CTAs) are needed. However, to the best of our knowledge, the supporting work on this topic has not yet been performed. In this work, a new class of cobaltocenium-labeled CTAs were prepared. These CTAs show excellent control for the polymerization of different monomers, including styrene, acrylate, methacrylate and acid. Distinct photophysical behavior and redox properties were also observed, which resulted from the cationic cobaltocene unit in the specific positions of the polymer chains, whereas the bulk behavior of polymer like thermal properties were unaffected.

### 2. Experimental sections

### 2.1. Materials

Thionyl chloride (SOCl<sub>2</sub>, 98%), dry triethylamine (TEA, 99%), dry ethylene glycol (99%), sodium tetraphenylboron (NaBPh4, 99%), 4cyano-4-((phenylcarbonothioyl)thio)pentanoic acid (98%), 4-dimethylaminopyridine (DMAP, 98%) and dicyclohexylcarbodiimide (DCC, 98%) were purchased from Sigma-Aldrich and used as received. Cobaltocenium hexafluorophosphate, 1,1'-cobaltocenium dicarboxylic acid hexafluorophosphate, 1-cobaltoceniummonocarboxylic acid hexafluorophosphate were prepared based on previous works [28]. 2,2-Azobis(isobutyronitrile) (AIBN) and azobis(1-cyclohexanenitrite) (ACHN) were recrystallized from dry ethanol. Methyl methacrylate (MMA, 99%), methyl acrylate (MA, 99%), 2-(dimethylamino)ethyl methacrylate (DMAEMA, 99%), methacrylic acid (MAA, 99%) and styrene (St, 99%) were passed through basic alumina columns before use. All solvents used for reaction were thoroughly dried unless otherwise stated. All the synthetic procedures were carried out under N2-protected conditions unless otherwise stated.

# 2.2. Characterization instruments

 $^1\mathrm{H}$  NMR (300 MHz, 400 MHz),  $^{13}\mathrm{C}$  NMR (75 MHz, 100 MHz) spectra were recorded by using a Bruker Avance III HD 300 or 400 spectrometer. The chemical shifts are reported with respect to CHCl<sub>3</sub>/CDCl<sub>3</sub> ( $\delta(^{1}\text{H}) =$ 7.26 ppm,  $\delta(^{13}\text{C}) = 77.0$  ppm), CH<sub>3</sub>CN/CD<sub>3</sub>CN ( $\delta(^{1}\text{H}) = 1.94$  ppm,  $\delta(^{13}\text{C}) = 1.32 \text{ ppm}$ ) and DMSO/DMSO- $d_6 (\delta(^{1}\text{H}) = 2.50 \text{ ppm})$ . ESI mass spectra were collected by a Waters Micromass Q-Tof mass spectrometer which utilized a positive-ion electrospray as the ionization source. Cyclic voltammograms (CV) were recorded by a CHI600E Electrochemical Analyzer/Workstation at a scan rate of 100 mV/s in dimethyl formamide (DMF) solution by using 0.1 M tetra-n-butylammonium hexafluorophosphate (TBAPF<sub>6</sub>) as the supporting electrolyte, glassy carbon as the working electrode, platinum as the counter electrode, and a silver/silver chloride (Ag/AgCl) electrode as the standard reference electrode. UV-Vis spectra were collected by a Shimadzu UV-2450 spectrophotometer using THF as solvent with a scan wavelength range of 200 nm to 600 nm. Morphology test were carried out by using atomic force microscopy (AFM). AFM images were collected from a Bruker Multimode Nanoscope V system via a tapping mode. The measurements were conducted using silicon cantilevers with a nominal spring constant at 20-80 N/m and a resonance frequency at 230-410 kHz. The polymer films used for AFM test were prepared via spin-coating. The films were supported on silicon wafers and dried at room environment. Differential scanning calorimeter (DSC) measurements were conducted on a Mettler-Toledo DSC1 DSC instrument using indium and zinc as internal references under nitrogen protection, the heating and cooling rate was fixed at 10  $^{\circ}$ C/min. The glass transition temperature ( $T_g$ ) was determined based on STARe method. The curves were recorded based on the second

heating scan. Thermogravimetric analysis (TGA) was conducted by using a Netzsch TG 209 F1 system (Netzsch Instruments), ramping from 30 to 700  $^{\circ}$ C at 20 K/min under nitrogen protection. The decomposition temperature ( $T_d$ ) was determined based on the peak value from the first derivative of the weight-temperature curve.

### 3. Results and discussion

### 3.1. Synthesis of cobaltocenium-labeled CTAs

4-Cyano-4-((phenylcarbonothioyl)thio)pentanoic acid has been well established to show excellent control over methacrylates, styrene, acrylates and others [37-39]. Here, 4-cyano-4-((phenylcarbonothioyl) thio)pentanoic acid was selected as the CTA and conjugate with cobaltocenium moieties. Synthesis of cobaltocenium-labeled CTAs was carried out with the use of cobaltocenium acyl chloride, which has been demonstrated to show high reactivity towards alcohols [21,40]. Therefore, the carboxylic acid group of 4-cyano-4-((phenylcarbonothioyl) thio)pentanoic acid was first transformed into hydroxyl functionality by undergoing an esterification reaction with ethylene glycol (Scheme 1). Then, monofunctional cobaltocenium-labeled CTA (mono-Cc-CTA) was synthesized by an esterification reaction between hydroxyethyl 4-cyano-4-(phenylcarbonothioylthio)pentanoate and freshly prepared monosubstituted cobaltocenium acyl chloride under the catalysis of trimethylamine in acetonitrile solution at room temperature. Similarly, difunctionalized cobaltocenium-labeled CTA (di-Cc-CTA) was prepared from disubstituted cobaltocenium acyl chlorides. The target products were easily separated by precipitation into ether.

Fig. 1a shows the <sup>1</sup>H NMR spectrum obtained for the mono- and difunctional cobaltocenium-labeled CTAs. Signals between 8.2 ppm and 7.0 ppm correspond to aromatic protons from the benzyl dithioester. The peaks between 6.5 ppm and 5.7 ppm are consistent with characteristic cyclopentadienyl (Cp) protons: mono-Cc-CTA shows three characteristic peaks, and di-Cc-CTA shows two characteristic peaks. All the other protons can be clearly assigned from the measures NMR spectra, and the integration matches well with theoretical values, indicating a high purity for the target products. <sup>13</sup>C NMR spectra in Fig. 1b further confirm the structure of these two cobaltocenium-labeled CTAs. Peaks with a chemical shift of ~223 ppm indicate the characteristic peaks of carbon from the dithioesters. The peaks at  $\sim$ 90 ppm correspond to the characteristic peaks of Cp. The identity of cobaltocenium-labeled CTAs was also confirmed by high-resolution electrospray mass spectra (Figs. S11 and S16). Mono-Cc-CTA shows a mass/charge ratio of 538.0551, consistent with a theoretical mass/charge ratio of 538.0552 with the loss of counterions during measurements. For di-Cc-CTA, the high-resolution mass spectrum shows a mass/charge ratio of 887.0998, which is in good agreement with the theoretical ratio of 887.0994. Therefore, both cobaltocenium-labeled CTAs were successfully prepared by a straightforward esterification reaction with high purity and high vields.

Cobaltocenium-labeled CTAs belong to organometallic electrolytes, with unique counterion-dependent physiochemical properties [41]. Here, we choose mono-Cc-CTA as an example. Tetraphenylborate (BPh4) was chosen as the counterion to replace the hexafluorophosphate ion (PF<sub>6</sub>) since the former usually shows stronger binding energy with the positively charged cobaltocenium moieties [4]. Additionally, the hydrophobicity of the cobaltocenium-labeled CTA can be finely tuned. The ion-exchange was proceeded by slowly adding mono-Cc-CTA into a methanol solution containing NaBPh<sub>4</sub>. Precipitation of a yellowish solid was subsequently observed, demonstrating the change of the solubility of the CTA after ion exchange. The product (abbreviated as mono--Cc-CTA-BPh<sub>4</sub>) shows good solubility in dichloromethane, whereas mono-Cc-CTA shows poor solubility in dichloromethane before ion exchange, indicating the special counterion-dependent solubility. <sup>1</sup>H NMR shows the explicit structure of the product with the BPh<sub>4</sub> counterion (Fig. S17) and <sup>19</sup>F NMR indicates the complete removal of PF<sub>6</sub> (Fig. S1).

Scheme 1. Synthesis of (a) terminal and (b) center cobaltocenium-labeled CTAs and polymers.

# 3.2. Kinetic studies

To evaluate the controllability of cobaltocenium-labeled CTAs for the polymerization of traditional monomers (e.g., MMA, MA, St, MAA and DMAEMA), kinetic studies were carried out. We conducted polymerization of MMA in DMF solution (monomer/solvent = 1:1 w/w) with a feed molar ratio of [monomer]: [CTA]: [AIBN] = 200: 1: 0.3. The polymerization temperature was fixed at 70 °C. The reaction conversion was calculated from  $^1\text{H}$  NMR analyses through comparing the integration areas between the polymers and monomers at different time intervals. As shown in Fig. 2a, a linear relationship for the semilogarithmic plots of  $\ln([\text{M}]_0/[\text{M}]_t)$  versus polymerization time mediated by mono-Cc-CTA is observed for the MMA system, indicating that the polymerization of MMA follows a controlled/living manner.

We then carried out a kinetic study of MA by using mono-Cc-CTA under the same experimental conditions used for MMA. The green line (Fig. 2a) that represents the polymerization kinetics of MA also exhibits a linear relationship between the reaction time and  $ln([M]_0/[M]_t)$ , whereas the rate of polymerization almost decreases to half that of MMA. The conversion of MMA reaches 50% at approximately 2 h, but it takes 4 h for MA to reach a comparable conversion. This result is reasonable due to the slower propagation rate of polyacrylyl radicals compared to that of the polymethacrylyl radicals [37].

Following the same procedure used for the kinetic study of MMA and MA, the polymerization of styrene was investigated. However, no polymer products were observed even after polymerization for 6 h, which can be attributed to the significantly slow rate of chain growth for styrene monomers. Therefore, we tried to increase the rate of polymerization by combining several settings: increasing the reaction temperature from 70  $^{\circ}\text{C}$  to 90  $^{\circ}\text{C}$ , increasing the monomer concentration from 50% to 90% (trace amount of DMF is needed to dissolve the CTA),

increasing the feed ratio of the initiator from 0.3 eq to 0.5 eq and changing the initiator from AIBN to ACHN, which has a longer half-life time [42]. After the reaction proceeds for 12 h, the polymerization conversion reaches 36%. Although the fraction of CTA in our system is higher (0.5 eq) than normal (usually less than 0.3 eq) during RAFT polymerization, it still shows good control over styrene monomers, as indicated from the blue line in Fig. 2a. Taken together, the synthesized mono-Cc-CTA is highly robust for controlling the RAFT polymerization process for a series of monomers, including MMA, MA and styrene. Previous work using site-specific ATRP to prepare terminated cobaltocenium-labeled PMMA showed nonliving polymerization kinetics but significant chain termination [21]. Here, site-specific RAFT polymerization shows superior controllability for site-specific ATRP in the preparation of terminated cobaltocenium-labeled polymers. PMMA, PMA and PS belong to hydrophobic polymers, the mono-Cc-CTA was also demonstrated to show good control over water-soluble monomers like MAA and DMAEMA (Fig. 2a), yielding hydrophilic polymers.

For di-Cc-CTA, as evidenced by the linear relationship between ln ([M] $_0$ /[M] $_t$ ) and reaction time (Fig. 2b), the RAFT polymerization process for these five monomers also follows a controlled/living manner. Then, the cobaltocenium moieties are dictated to be placed in the very middle of the polymer chains. For both CTAs, the polymerization rate follows the same relationship of MAA > MMA > DMAEMA > MA > St.

# 3.3. Preparation of cobaltocenium-labeled polymers with high molecular weights

For site-specific labeled polymers, in many cases, high molecular weight is necessary for a variety of applications [43,44]. To prepare a polymer with high molecular weight via RAFT polymerization is not easy since it requires a longer reaction time and an external source of

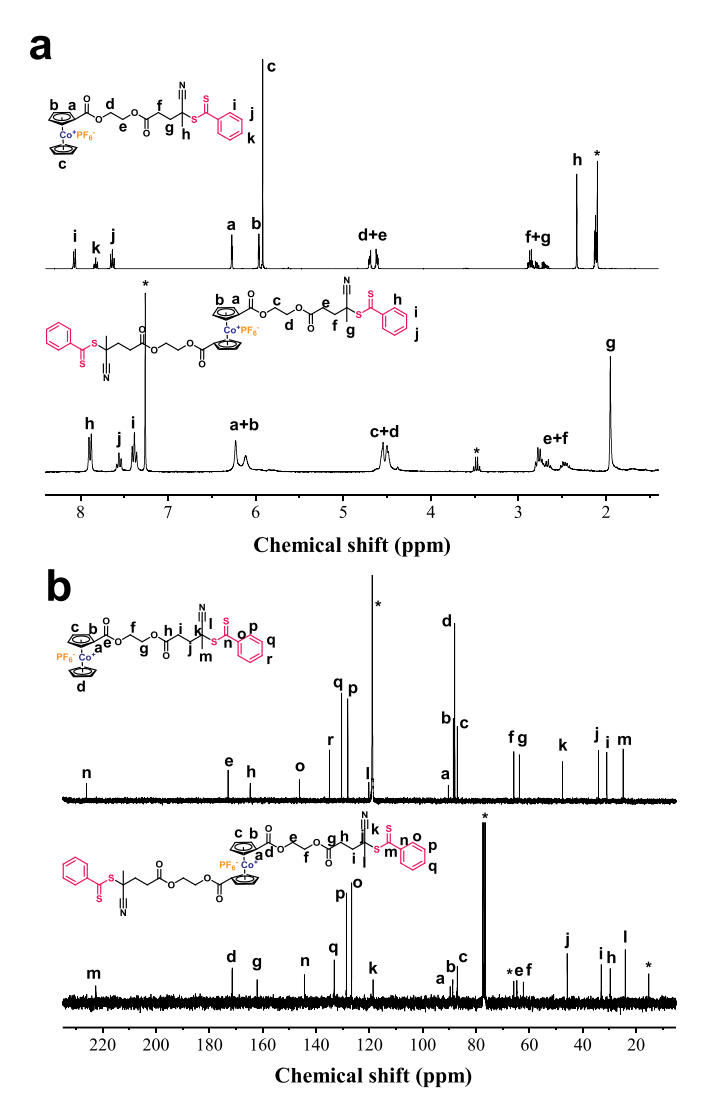
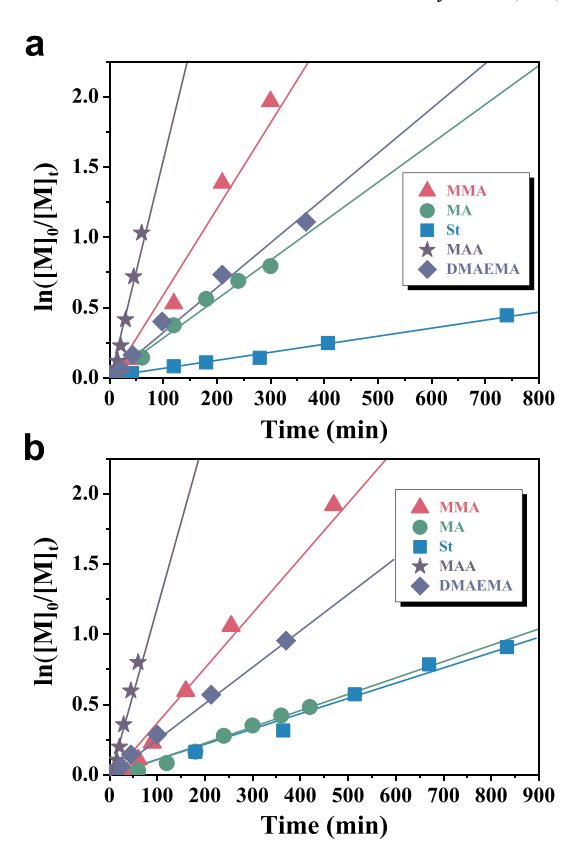


Fig. 1.  $^{1}\mathrm{H}$  NMR spectra (a) and  $^{13}\mathrm{C}$  NMR spectra (b) of mono-Cc-CTA and di-Cc-CTA.

radicals is always required to initiate and maintain polymerization as the conversion proceeds. However, initiators with a short half-life time, e.g., AIBN (half-life time of 5 h at 70 °C), are not sufficient for generating free radicals at longer reaction times. Here, we chose ACHN as an initiator to carry out the polymerization of MMA at 90 °C with molar ratios of [MMA]:[mono-Cc-CTA]:[ACHN] = 1000:1:0.3. The reaction was quenched at 200 min when the reaction mixture became very viscous at a conversion of 68% based on <sup>1</sup>H NMR analysis. After purification, the protons in the product well correspond to the PMMA backbone, as shown in Fig. 3a. A zoomed-in view of the high-resolution <sup>1</sup>H NMR spectrum from 4.0 ppm to 8.0 ppm clearly shows the characteristic cobaltocenium peaks (5.8 ppm-6.3 ppm) and dithioester terminal groups (7.3 ppm-8.0 ppm). Additionally, the integration matches their structural stoichiometry well. The yielded polymer (Cc-PMMA) shows a degree of polymerization (DP) of ~700 based on terminal group analysis. Due to the strong electrostatic binding between the cobaltocenium moieties and gel permeation chromatography (GPC) columns, it is very challenging to calibrate the peak signal from the cobaltocenium-labeled polymers [35,45]. Nevertheless, the DP value is consistent with the NMR conversion data, indicating that the polymerization follows a controlled manner.

Dithiobenzoate as a terminal group is not stable under heat and can be potentially toxic, and can be removed from polymer chains by heating the mixture of polymer with excess AIBN in toluene, yielding a



**Fig. 2.** Semilogarithmic plots of polymerization for different monomers by (a) mono-Cc-CTA, (b) di-Cc-CTA.  $[M]_0$  is the monomer concentration at the very beginning, and  $[M]_t$  is the monomer concentration at a given time.

cyano group terminated polymer [46,47]. After purification, the color of the polymer changes from light pink to white (Fig. S2); in addition, the polymer shows complete loss of the characteristic peak due to the dithiobenzoate; however, the cobaltocenium moiety remains unaffected (Fig. 3b and e).

For di-Cc-CTA, when the molar feed ratio was fixed as [MMA]:[di-Cc-CTA]:[ACHN] = 2000:1:0.6, di-Cc-CTA was anticipated to yield double the molecular weight compared to its mono-functional counterpart due to the concurrent polymerization of essentially all of the MMA monomers. The polymerization was conducted at 90 °C for 500 min until solidification with a conversion of 73%. The  $^1\text{H}$  NMR analysis in Fig. 3c shows that the yielded polymer has a DP of 1400 based on terminal group analysis ( $M_n=141,100$  Da). The millesimal molar ratio of the PF $_6^-$  counterion on the PMMA backbone can be clearly observed from the  $^{19}\text{F}$  NMR spectra for both end-labeled and center-labeled polymers, as shown in Fig. 3d and 3f, respectively, indicating the high stability of the cobaltocenium hexafluorophosphate complex during RAFT polymerization. However, the ATRP process is inaccessible, as the counterion in the latter case might exchange with the halide ion from the copper catalyst [21].

# 3.4. Photophysical properties

To further understand the photophysical properties of these cobaltocenium-labeled CTAs and polymers, we utilized UV–Vis spectroscopy to monitor the dithiobenzoate and cobaltocenium moieties in these labeled structures. For cobaltocenium-labeled CTAs, monofunctional substituents show a dominant peak at a wavelength of 273 nm (Fig. 4a), consistent with the n- $\pi$ \* transitions from cobaltocenium [21]. However, this peak shifts to 281 nm for di-Cc-CTA, which can be rationalized by the electron-withdrawing effect due to the two ester substituents on the Cp rings. A d-d\* transition peak at 409 nm serves as

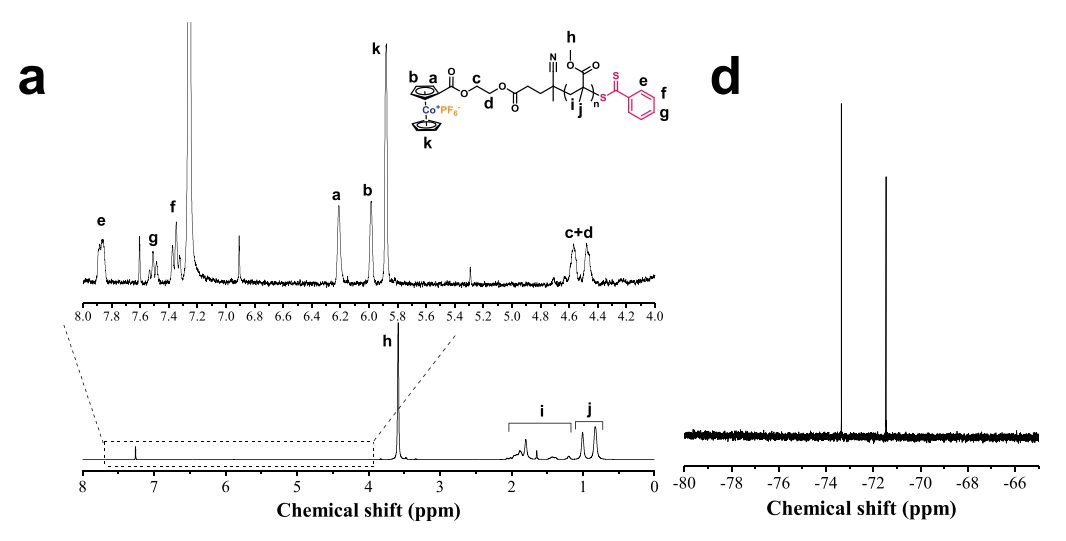
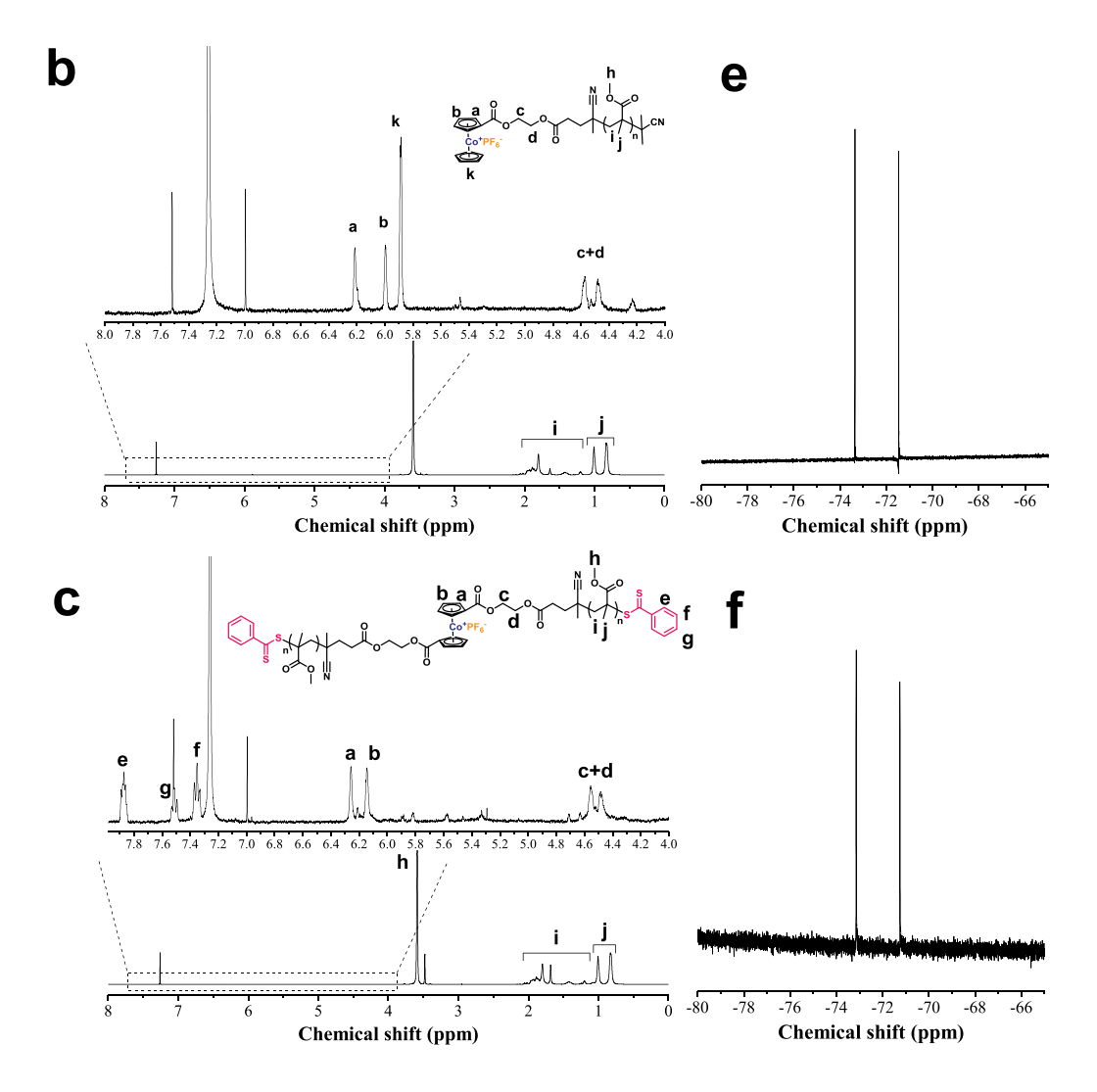


Fig. 3. <sup>1</sup>H NMR spectra for (a) cobaltocenium-labeled PMMA with terminal function (Cc-PMMA), (b) cobaltocenium-labeled PMMA without dithiobenzoate group (Cc-PMMA-CN), (c) cobaltocenium-labeled PMMA with center function (PMMA-Cc-PMMA). <sup>19</sup>F NMR spectra for (d) cobaltocenium-labeled PMMA with terminal function (Cc-PMMA), (e) cobaltocenium-labeled PMMA without a dithiobenzoate group (Cc-PMMA-CN), and (f) cobaltocenium-labeled PMMA with center function (PMMA-Cc-PMMA).



another evidence for a cobaltocenium motif [21]. The absorption characteristics of the  $\pi^*$ - $\pi^*$  transition (302 nm) and n- $\pi^*$  transition (518 nm) of the thiocarbonyl bond confirm the presence of dithiobenzoate moieties in the structure of the CTAs [48].

For cobaltocenium-labeled polymers, the characteristic peak shapes and positions for the cobaltocenium moiety are pretty similar to those of small molecules, as shown in Fig. 4b, demonstrating the successful incorporation of cobaltocenium groups into the polymer chains. When the dithiobenzoate group is removed from the PMMA backbone, the absorption characteristics due to the  $\pi^*$ - $\pi^*$  transition (302 nm) and n- $\pi^*$  transition (518 nm) of the thiocarbonyl bond (blue curve in Fig. 4b) disappear completely compared to the precursor (green curve in

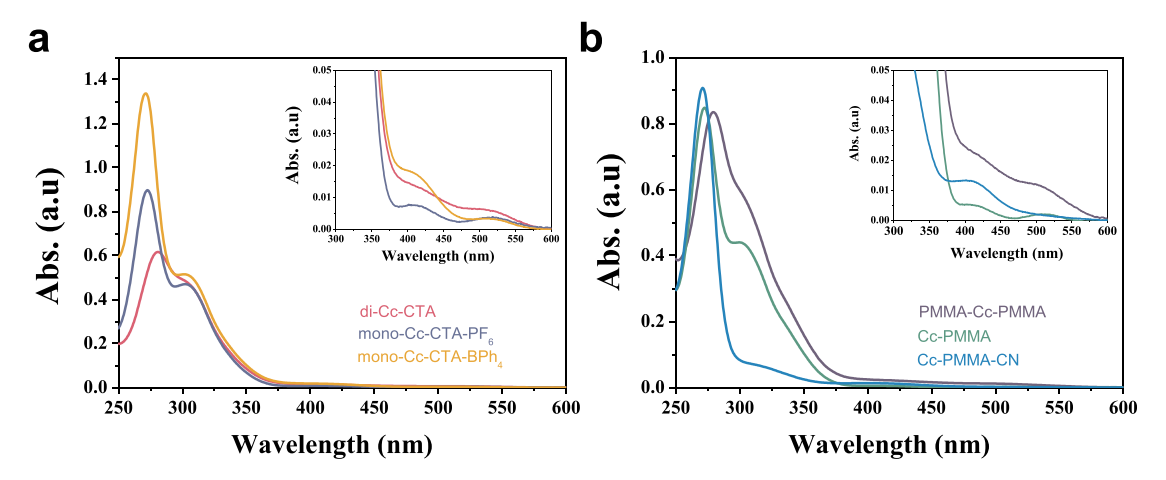
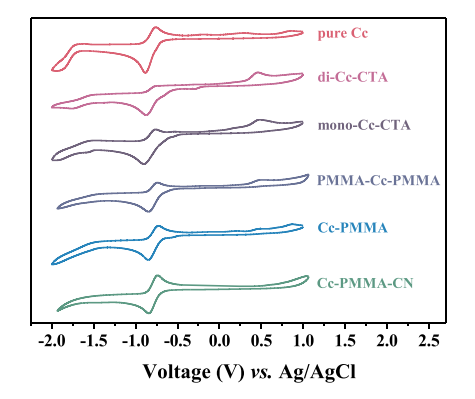


Fig. 4. UV-Vis spectra for (a) cobaltocenium-labeled CTAs and (b) cobaltocenium-labeled polymers. Inset images show a zoomed-in region from 300 nm to 600 nm.

Fig. 4b). Since the UV–Vis absorption of the cobaltocenium-labeled polymers is largely affected by the substituents directly linked to Cp rings, the absorption wavelengths and intensities show no difference for the cobaltocenium-labeled polymers with the molecular weight in the range of 6000 Da to 70,000 Da (Fig. S3).

### 3.5. Electrochemical properties

The electrochemical properties of cobaltocenium-labeled CTAs and polymers were studied using cyclic voltammetry (CV) in DMF solution with tetra-n-butylammonium hexafluorophosphate (TBAPF<sub>6</sub>) as supporting electrolyte. A silver/silver chloride (Ag/AgCl) electrode was used as a reference electrode to determine the electrochemical potentials. As Fig. 5 shows, cobaltocenium-labeled CTAs both show a redox process with both reduction and oxidation potential at approximately -0.89 V and -0.76 V, respectively, due to the reversible electrochemistry of the cobaltocenium moiety. The reduction peak current is higher than the oxidation peak current. In the case of cobaltocenium-labeled polymers, the redox process is more reversible, largely due to the better solubility of the polymer in DMF solution [21]. Generally, the electrochemical potentials can be tuned by the substituents linked to the Cp of the metallocenes [29,49,50]. For ferrocene, the electrochemical potentials of electron-withdrawing groups, e.g., ester groups, can show a pronounced positive shift when they are linked to Cp rings, making the ferrocene structure even less stable in an oxidative environment [16]. Interestingly, the electron-withdrawing ester substituents on cobaltocenium do not significantly affect the electrochemical potentials since the redox potentials for di-substituted and mono-substituted substituents are comparable, demonstrating the superior redox stability of cobaltocenium-labeled polymers. The electrochemical properties of the



**Fig. 5.** Cyclic voltammetry plots for pure cobaltocenium, cobaltocenium-labeled CTAs and polymers.

cobaltocenium-labeled polymers are not affected by the molecular weight in the range of 6000 Da to 70,000 Da (Fig. S4).

### 3.6. Thermal properties and morphology study

Metallocenes are known to show high thermal stability [51]. The incorporation of metallocene motifs into polymer backbone might influence the thermal properties of the material, including glass transition temperatures ( $T_{\rm g}$ ) and decomposition temperatures ( $T_{\rm d}$ ). Here, we investigated the thermal properties of cobaltocenium-labeled PMMA. The molecular weights of blank PMMA, Cc-PMMA and PMMA-Cc-PMMA were fixed the same (70,000 Da). As shown in Fig. 6, all three samples show indistinguishable  $T_{\rm g}$  (121 °C) and  $T_{\rm d}$  (370 °C). Given the low labeling ratio ( $\sim$ 0.14% mole ratio) of cobaltocenium moieties on the backbone of PMMA, the yielded difference in the thermal properties of bulk material is negligible.

Another concern is that the cobaltocenium moieties might aggregate together toward phase-separation with cationic metallocene motifs distributed in one domain, whereas the polymer backbone will be enriched in the other domain. To evaluate the morphology of the cobaltocenium-labeled polymers, three PMMA films were prepared via a spin-coating strategy. As shown in Fig. S5, homogenous morphology of cobaltocenium-labeled PMMA is confirmed compared to blank PMMA. Phase-separation only happens at higher labeling ratio [52]. Collectively, the cobatocenium motifs on the polymer chains only act as probes but do not influence the bulk properties of the material.

# 4. Conclusions

In summary, two novel cobaltocenium-labeled CTAs were synthesized and thoroughly characterized. Based on the chemical structures of the CTAs, cobaltocenium groups can be selectively located in the center or at the terminals of polymer chains. Both di- and mono-functionalized CTAs show excellent control for the polymerization of a series of monomers, including hydrophobic ones (MMA, MA and St) and hydrophilic ones (MAA and DMAEMA). The unique counterion-dependent solubility of cobaltocenium also endows the CTA with adjustable solubility. Additionally, the molecular weight of the cobaltocenium-labeled polymer can reach over 100,000 Da via robust control of the difunctional CTA. The thermal and chemical liable dithiobenzoate moiety at one polymer chain end can be easily removed with no influence on the cobaltocenium moiety. All resultant polymers show characteristic UV-Vis absorption and redox-active properties due to the cobaltocenium probe. The morphology and thermal properties of bulk polymers are not affected by the incorporation of cobaltocenium motifs due to the low labeling ratio. This work provides new efforts towards the controlled synthesis of charged metallopolymers. These site-

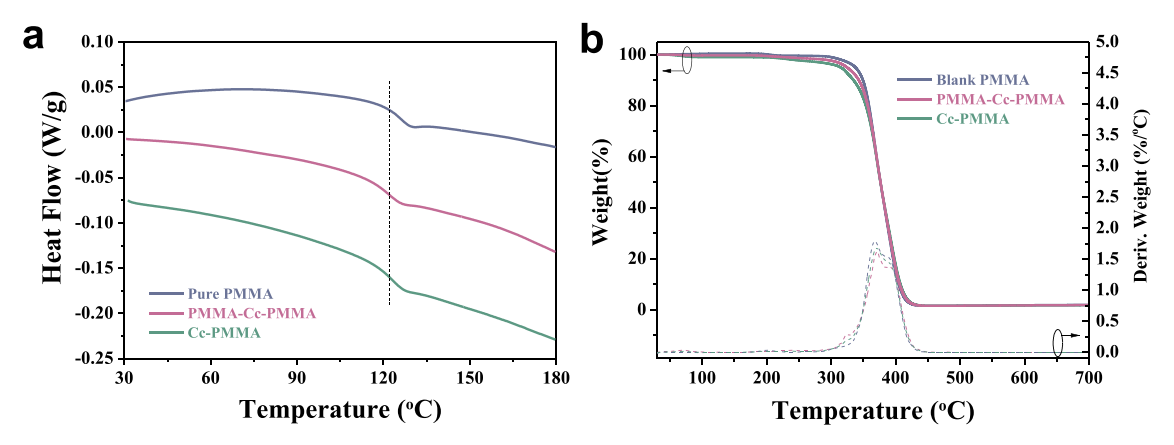


Fig. 6. (a) DSC heating scans of PMMA samples. (b) Thermogravimetric analysis of PMMA samples. The molecular weight for each sample is 70,000 Da.

specific labeled metallopolymers are envisaged to act as versatile, redox-responsive, optically active and stress-responsive materials for applications in electrochemical sensing, bioimaging and mechanochemical sensing.

#### CRediT author statement

Ye Sha: Conceptualization; Roles/Writing - original draft; Methodology. Tianyu Zhu: Writing - review & editing; Visualization. Md Anisur Rahman: Software. Yujin Cha: Formal analysis. Jihyeon Hwang: Data curation. Zhenyang Luo: Investigation; Resources. Chuanbing Tang: Funding acquisition; Project administration; Supervision; Validation.

### Declaration of competing interest

The authors declare that they have no known competing financial interests or personal relationships that could have appeared to influence the work reported in this paper.

## Acknowledgments

This study is partially supported by the National Institutes of Health (R01AI120987). Partial support from the National Science Foundation EPSCoR Program (NSF Award # OIA-1655740) is also acknowledged.

### Appendix A. Supplementary data

Supplementary data to this article can be found online at https://doi.org/10.1016/j.polymer.2019.122095.

### References

- [1] R.L.N. Hailes, A.M. Oliver, J. Gwyther, G.R. Whittell, I. Manners, Polyferrocenylsilanes: synthesis, properties, and applications, Chem. Soc. Rev. 45 (19) (2016) 5358–5407.
- [2] L. Zhao, X. Liu, L. Zhang, G. Qiu, D. Astruc, H. Gu, Metallomacromolecules containing cobalt sandwich complexes: synthesis and functional materials properties, Coord. Chem. Rev. 337 (2017) 34–79.
- [3] Y. Wang, D. Astruc, A.S. Abd-El-Aziz, Metallopolymers for advanced sustainable applications, Chem. Soc. Rev. 48 (2019) 558–636.
- [4] T. Zhu, Y. Sha, J. Yan, P. Pageni, M.A. Rahman, Y. Yan, C. Tang, Metallopolyelectrolytes as a class of ionic macromolecules for functional materials, Nat. Commun. 9 (2018), 4329.
- [5] Y. Yan, J. Zhang, L. Ren, C. Tang, Metal-containing and related polymers for biomedical amplications. Chem. Soc. Rev. 45 (19) (2016) 5232–5263.
- [6] M. Gallei, C. Ruttiger, Recent trends in metallopolymer design: redox-controlled surfaces, porous membranes, and switchable optical materials using ferrocenecontaining polymers, Chem. Eur J. 24 (40) (2018) 10006–10021.
- [7] P. Wei, X. Yan, F. Huang, Supramolecular polymers constructed by orthogonal selfassembly based on host-guest and metal-ligand interactions, Chem. Soc. Rev. 44 (3) (2015) 815–832.

- [8] A. Voevodin, L.M. Campos, X. Roy, Multifunctional vesicles from a self-assembled cluster-containing diblock copolymer, J. Am. Chem. Soc. 140 (16) (2018) 5607–5611.
- [9] H. Zhang, H. Zhao, K. Zhuo, Y. Hua, J. Chen, X. He, W. Weng, H. Xia, "Carbolong" polymers with near infrared triggered, spatially resolved and rapid self-healing properties, Polym. Chem. 10 (3) (2019) 386–394.
- [10] A. Alkan, F.R. Wurm, Water-soluble metallocene-containing polymers, macromol, Rapid Commun. 37 (18) (2016) 1482–1493.
- [11] D. Astruc, Why is ferrocene so exceptional? Eur. J. Inorg. Chem. 1 (2017) 6–29.
- [12] A.S. Abd-El-Aziz, C. Agatemor, N. Etkin, Antimicrobial resistance challenged with metal-based antimicrobial macromolecules, Biomaterials 118 (2017) 27–50.
- [13] C. Hardy, J. Zhang, Y. Yan, L. Ren, C. Tang, Metallopolymers with transition metals in the side-chain by living and controlled polymerization techniques, Prog. Polym. Sci. 39 (10) (2014) 1742–1796.
- [14] K.A. Williams, A.J. Boydston, C.W. Bielawski, Main-chain organometallic polymers: synthetic strategies, applications, and perspectives, Chem. Soc. Rev. 36 (5) (2007) 729–744.
- [15] P. Nguyen, P. Gomez-Elipe, I. Manners, Organometallic polymers with transition metals in the main chain, Chem. Rev. 99 (6) (1999) 1515–1548.
- [16] Y. Sha, Y. Zhang, T. Zhu, S. Tan, Y. Cha, S.L. Craig, C. Tang, Ring-closing metathesis and ring-opening metathesis polymerization toward main-chain ferrocene-containing polymers, Macromolecules 51 (22) (2018) 9131–9139.
- [17] H. Gu, R. Ciganda, P. Castel, S. Moya, R. Hernandez, J. Ruiz, D. Astruc, Tetrablock metallopolymer electrochromes, Angew. Chem. Int. Ed. 57 (8) (2018) 2204–2208.
- [18] R.A. Musgrave, A.D. Russell, D.W. Hayward, G.R. Whittell, P.G. Lawrence, P. J. Gates, J.C. Green, I. Manners, Main-chain metallopolymers at the static-dynamic boundary based on nickelocene, Nat. Chem. 9 (8) (2017) 743–750.
- [19] Y. Yan, J. Zhang, Y. Qiao, M. Ganewatta, C. Tang, Ruthenocene-containing homopolymers and block copolymers via ATRP and RAFT polymerization, Macromolecules 46 (22) (2013) 8816–8823.
- [20] Y. Sha, A. Rahman, T. Zhu, Y. Cha, C. McAlister, C. Tang, ROMPI-CDSA: ring-opening metathesis polymerization induced-crystallization-driven self-assembly of metallo-block copolymers, Chem. Sci. 10 (2019) 9782–9787.
- [21] L. Ren, J. Zhang, C.G. Hardy, D. Doxie, B. Fleming, C. Tang, Preparation of cobaltocenium-labeled polymers by atom transfer radical polymerization, Macromolecules 45 (5) (2012) 2267–2275.
- [22] Y. Li, N.L. Haworth, L. Xiang, S. Ciampi, M.L. Coote, N. Tao, Mechanical stretching-induced electron-transfer reactions and conductance switching in single molecules, J. Am. Chem. Soc. 139 (41) (2017) 14699–14706.
- [23] M. Di Giannantonio, M.A. Ayer, E. Verde-Sesto, M. Lattuada, C. Weder, K. M. Fromm, Triggered metal ion release and oxidation: ferrocene as new mechanophore in polymers, Angew. Chem. Int. Ed. 57 (2018) 11445–11450.
- [24] Y. Sha, Y. Zhang, E. Xu, C.W. McAlister, T. Zhu, Stephen L. Craig, C. Tang, Generalizing metallocene mechanochemistry to ruthenocene mechanophores, Chem. Sci. 10 (2019) 4959–4965.
- [25] Y. Sha, Y. Zhang, E. Xu, Z. Wang, T. Zhu, S.L. Craig, C. Tang, Quantitative and mechanistic mechanochemistry in ferrocene dissociation, ACS Macro Lett. 7 (10) (2018) 1174–1179.
- [26] N. Zhou, Z. Zhang, J. Zhu, Z. Cheng, X. Zhu, RAFT polymerization of styrene mediated by ferrocenyl-containing RAFT agent and properties of the polymer derived from ferrocene, Macromolecules 42 (12) (2009) 3898–3905.
- [27] Y. Yan, T.M. Deaton, J. Zhang, H. He, J. Hayat, P. Pageni, K. Matyjaszewski, C. Tang, Syntheses of monosubstituted rhodocenium derivatives, monomers, and polymers, Macromolecules 48 (6) (2015) 1644–1650.
- [28] L. Ren, C. Hardy, C. Tang, Synthesis and solution self-assembly of side-chain cobaltocenium-containing block copolymers, J. Am. Chem. Soc. 132 (26) (2010) 8874–8875.
- [29] C. Hardy, L. Ren, T. Tamboue, C. Tang, Side-chain ferrocene-containing (Meth) acrylate polymers: synthesis and properties, J. Polym. Sci. A-Polym. Chem. 49 (6) (2011) 1409–1420.
- [30] S. Zhai, J. Shang, D. Yang, S. Wang, J. Hu, G. Lu, X. Huang, Successive SET-LRP and ATRP synthesis of ferrocene-based PPEGMEA-g-PAEFC well-defined

- amphiphilic graft copolymer, J. Polym. Sci. A-Polym. Chem. 50 (4) (2012) 811–820.
- [31] C. Feng, Z. Shen, D. Yang, Y. Li, J. Hu, G. Lu, X. Huang, Synthesis of well-defined amphiphilic graft copolymer bearing poly(2-acryloyloxyethyl ferrocenecarboxylate) side chains via successive SET-LRP and ATRP, J. Polym. Sci. A-Polym. Chem. 47 (17) (2009) 4346–4357.
- [32] B.Y. Kim, E.L. Ratcliff, N.R. Armstrong, T. Kowalewski, J. Pyun, Ferrocene functional polymer brushes on indium tin oxide via surface-initiated atom transfer radical polymerization, Langmuir 26 (3) (2010) 2083–2092.
- [33] J. Elbert, M. Gallei, C. Ruettiger, A. Brunsen, H. Didzoleit, B. Stuehn, M. Rehahn, Ferrocene polymers for switchable surface wettability, Organometallics 32 (20) (2013) 5873–5878.
- [34] P. Yang, P. Pageni, M.P. Kabir, T. Zhu, C. Tang, Metallocene-containing homopolymers and heterobimetallic block copolymers via photoinduced RAFT polymerization, ACS Macro Lett. 5 (11) (2016) 1293–1300.
- [35] Y. Yan, J. Zhang, Y. Qiao, C. Tang, Facile preparation of Cobaltocenium-Containing polyelectrolyte via click chemistry and RAFT polymerization, Macromol. Rapid Commun. 35 (2) (2014) 254–259.
- [36] J. Zhang, L. Ren, C.G. Hardy, C. Tang, Cobaltocenium-containing methacrylate homopolymers, block copolymers, and heterobimetallic polymers via RAFT polymerization, Macromolecules 45 (17) (2012) 6857–6863.
- [37] G. Moad, E. Rizzardo, S.H. Thang, Radical addition-fragmentation chemistry in polymer synthesis, Polymer 49 (5) (2008) 1079–1131.
- [38] G. Moad, E. Rizzardo, S.H. Thang, Living radical polymerization by the RAFT process, Aust. J. Chem. 58 (6) (2005) 379–410.
- [39] J. Chiefari, Y.K. Chong, F. Ercole, J. Krstina, J. Jeffery, T.P.T. Le, R.T. A. Mayadunne, G.F. Meijs, C.L. Moad, G. Moad, E. Rizzardo, S.H. Thang, Living free-radical polymerization by reversible addition-fragmentation chain transfer: the RAFT process, Macromolecules 31 (16) (1998) 5559–5562.
- [40] L. Ren, C.G. Hardy, S. Tang, D.B. Doxie, N. Hamidi, C. Tang, Preparation of sidechain 18-e cobaltocenium-containing acrylate monomers and polymers, Macromolecules 43 (22) (2010) 9304–9310.
- [41] J. Zhang, Y. Yan, M.W. Chance, J. Chen, J. Hayat, S. Ma, C. Tang, Charged metallopolymers as universal precursors for versatile cobalt materials, Angew. Chem. Int. Ed. 52 (50) (2013) 13387–13391.

- [42] M. Benaglia, J. Chiefari, Y.K. Chong, G. Moad, E. Rizzardo, S.H. Thang, Universal (switchable) RAFT agents, J. Am. Chem. Soc. 131 (20) (2009) 6914–6915.
- [43] M.M. Caruso, D.A. Davis, Q. Shen, S.A. Odom, N.R. Sottos, S.R. White, J.S. Moore, Mechanically-induced chemical changes in polymeric materials, Chem. Rev. 109 (11) (2009) 5755–5798.
- [44] B. Lee, Z. Niu, J. Wang, C. Slebodnick, S.L. Craig, Relative mechanical strengths of weak bonds in sonochemical polymer mechanochemistry, J. Am. Chem. Soc. 137 (33) (2015) 10826–10832.
- [45] Y. Cha, C. Jarrett-Wilkins, M.A. Rahman, T. Zhu, Y. Sha, I. Manners, C. Tang, Crystallization-driven self-assembly of metallo-polyelectrolyte block copolymers with a polycaprolactone core-forming segment, ACS Macro Lett. 8 (7) (2019) 835–840.
- [46] S. Perrier, P. Takolpuckdee, C.A. Mars, Reversible addition-fragmentation chain transfer polymerization: end group modification for functionalized polymers and chain transfer agent recovery, Macromolecules 38 (6) (2005) 2033–2036.
- [47] G. Moad, E. Rizzardo, S.H. Thang, End-functional polymers, thiocarbonylthio group removal/transformation and reversible addition-fragmentation-chain transfer (RAFT) polymerization, Polym. Int. 60 (1) (2011) 9–25.
- [48] K. Skrabania, A. Miasnikova, A.M. Bivigou-Koumba, D. Zehm, A. Laschewsky, Examining the UV-vis absorption of RAFT chain transfer agents and their use for polymer analysis, Polym. Chem. 2 (9) (2011) 2074–2083.
- [49] J. Langmaier, Z. Samec, V. Varga, M. Horáček, K. Mach, Substituent effects in cyclic voltammetry of titanocene dichlorides, J. Organomet. Chem. 579 (1) (1999) 348–355.
- [50] C.E. Zachmanoglou, A. Docrat, B.M. Bridgewater, G. Parkin, C.G. Brandow, J. E. Bercaw, C.N. Jardine, M. Lyall, J.C. Green, J.B. Keister, The electronic influence of ring substituents and ansa bridges in zirconocene complexes as probed by infrared spectroscopic, electrochemical, and computational studies, J. Am. Chem. Soc. 124 (32) (2002) 9525–9546.
- [51] A. Haaland, Molecular structure and bonding in the 3d metallocenes, Accounts Chem. Res. 12 (11) (1979) 415–422.
- [52] T. Zhu, S. Xu, A. Rahman, E. Dogdibegovic, P. Yang, P. Pageni, M.P. Kabir, X. Zhou, C. Tang, Cationic metallo-polyelectrolytes for robust alkaline anion-exchange membranes, Angew. Chem. Int. Ed. 57 (9) (2018) 2388–2392.